crystals

MDPI

*Article*

# Drug Repurposing for the Discovery of Potential Inhibitors Targeting DJ-1 (PARK7) Against Parkinson's Disease

**Taibah Aldakhil and Ali Altharawi ***

Department of Pharmaceutical Chemistry, College of Pharmacy, Prince Sattam Bin Abdulaziz University, Al-Kharj 11942, Saudi Arabia; t.aldakhil@psau.edu.sa
* Correspondence: a.altharawi@psau.edu.sa

**Abstract:** Parkinson's disease (PD) is a neurodegenerative disease characterized by increased movement dysfunction and cognitive loss. DJ-1 (PARK7) is an antioxidant that protects cells from oxidative stress, a major contributor to cellular damage and neurodegeneration in PD. Mutations in the DJ-1 gene reduce its neuroprotective ability contributing to PD onset and progression. The neuroprotective and antioxidant properties of DJ-1 make it a viable therapeutic target for developing novel PD therapeutics. A drug repurposing approach was applied to identify promising inhibitors for DJ-1. Three drugs—droxicam, pteroylglutamic acid, and niraparib—were identified based on their binding affinities and interactions. Further molecular dynamics simulations revealed that niraparib and pteroylglutamic acid were the most stable among the three complexes. Moreover, the binding strength of the complexes was confirmed by MMPBSA binding free energy analysis, with Niraparib (−13.50 kcal/mol) and pteroylglutamic Acid (−11.41 kcal/mol) as the most promising candidates. These results suggest that pteroylglutamic acid and niraparib may serve as useful DJ-1 inhibitors for PD-associated protein DJ-1. Further experimental validation and in vivo assessments are required to confirm the efficacy and safety of these drugs against PD.

**Keywords:** Parkinson's disease; neurodegenerative; oxidative stress; drugs; molecular dynamics simulations; neuroprotective

check for updates

Academic Editor: Emilio Parisini

Received: 17 December 2024
Revised: 21 February 2025
Accepted: 25 February 2025
Published: 28 February 2025

**Citation:** Aldakhil, T.; Altharawi, A. Drug Repurposing for the Discovery of Potential Inhibitors Targeting DJ-1 (PARK7) Against Parkinson's Disease. *Crystals* **2025**, *15*, 239. https://doi.org/10.3390/cryst15030239

**Copyright:** © 2025 by the authors. Licensee MDPI, Basel, Switzerland. This article is an open access article distributed under the terms and conditions of the Creative Commons Attribution (CC BY) license (https://creativecommons.org/licenses/by/4.0/).

## 1. Introduction

Parkinson's disease (PD) is a prevalent, progressive neurological movement disorder marked by motor symptoms such as slowed movement, tremor, rigidity, and postural instability. PD affects 1% of the population by the age of 65. Motor symptoms include slowness of movement, resting tremor, postural instability, and muscle rigidity, all of which are produced by dopaminergic neuron loss in the substantia nigra [1]. In addition to motor symptoms, PD includes non-motor symptoms such as rapid eye movement (REM), sleep disruption, and loss of olfaction, which can occur before motor symptoms. Most PD cases (90–95%) are sporadic, although 5–10% are hereditary and develop at an early age [2]. Early-onset Parkinson's disease (EOPD) has symptoms comparable to sporadic PD, but there are important fundamental distinctions. Mutations in D-related genes (PARK-genes) that are autosomal inherited can increase the risk of developing PD. So far, 23 PARK genes have been associated with PD [3]. DJ-1 has been linked to early-onset PD due to mutations [4]. These pathological mutations, including M26I, D149A, and L166A, result in the complete loss of DJ-1 expression or lead to the production of a non-functional protein, which both contribute to the development of PD [5]. DJ-1 also protects dopaminergic

neurons from the toxicity of rotenone [6]. Numerous structural, biochemical, and cellular studies have investigated its protective effect on dopaminergic [7–9].

The DJ-1 protein is made up of a single domain that has 198 amino acid residues and a molecular weight of about 20 kDa. This domain shares structural similarities with several bacterial enzyme families, such as ThiJ, which is involved in thiamine biosynthesis, and the Pfp1 protease [4]. Additionally, DJ-1 is homologous with the redox-sensitive chaperone YajL [10]. Numerous researchers determined the three-dimensional structure of DJ-1 by rigorous study a decade ago [7–9]. According to these investigations, DJ-1 adopts a compact globular fold and has an active site that is centered around the Cys106 residue. This residue is extremely reactive and prone to oxidation, making it an essential feature of the protein's functional site (Figure 1B). Furthermore, mutations in DJ-1, such as the Leu166 to Proline (L166P) substitution, have been linked to early-onset Parkinson's disease. The L166P mutation disrupts DJ-1's structural integrity, leading to protein destabilization and loss of function, which contributes to neurodegeneration [11]. Cys106 functions as an oxidative stress sensor. It is extremely reactive because of its side chain thiol group (-SH), which can oxidize to several states, such as sulfenic acid and sulfonic acid (highly oxidized), thus inactivating DJ-1. Due to this oxidation, DJ-1 is able to recognize and react to the increase in the reactive oxygen species (ROS), elevated in PD [12] (Figure 1A). Small molecules can be discovered to improve the activity or maintain the active state of DJ-1, enhancing neuroprotection. Olzmann et al., established that DJ-1 exists in solution as a stable dimer [11]. The importance of dimerization for DJ-1 function is further confirmed by the studies on the PD-associated L166P mutation, which prevents dimer formation. This mutation not only inhibits dimerization but also reduces DJ-1's neuroprotective action, demonstrating that the dimeric form of protein is critical for its biological function [11]. The neuroprotective properties of DJ-1 in counteracting oxidative stress have led to a significant interest in its potential as a therapeutic target for PD. Identifying molecules that stabilize or mimic DJ-1's antioxidant activity could provide therapeutic benefits in PD. Therapeutic modulation of DJ-1 could also protect against mitochondrial dysfunction, a hallmark of PD pathology. Developing therapies that enhance DJ-1's protective role or restore its function in mutated forms may offer new avenues for neuroprotection, potentially slowing PD progression [5].

Drug repurposing is cost-effective and time-efficient, as it builds on drugs with known safety profiles and manufacturing processes. Repurposed drugs can often move directly into testing for efficacy in new disease contexts, making this approach valuable for addressing diseases with limited therapeutic options [13]. DJ-1 is a relatively novel target compared to pathways like dopamine synthesis, GLP-1 receptors, or c-Abl kinase. DJ-1 is essential for protecting neurons against oxidative stress, mitochondrial dysfunction, and neuroinflammation, all of which are critical in PD progression [14]. Different drugs have been repurposed in order to combat PD as neuroprotective by targeting the PD pathogenesis pathways. Pagan et al. studied the safety and tolerability of the drug Nilotinib against PD by targeting tyrosine kinase Abl [5]. Athauda et al. investigated the effects of Exenatide, a GLP-1 receptor agonist initially used for diabetes, on motor and cognitive symptoms in Parkinson's disease (PD) patients [15]. Though several drugs have been repurposed to target different pathways involved in PD, DJ-1 remains an underexplored target. In this study, we focused on screening FDA-approved drugs from the DrugBank database to identify potential inhibitors of DJ-1 that could offer neuroprotective benefits in PD. The goal of this study is to find inhibitors that may directly improve the neuroprotective effects of DJ-1. Molecular dynamics simulations (MDSs) were used to evaluate the stability and interaction of the most promising compounds found during the first screening with DJ-1.

In addition, Molecular Mechanics Poisson–Boltzmann Surface Area (MMPBSA) was used to find the binding free energies of the selected drugs.

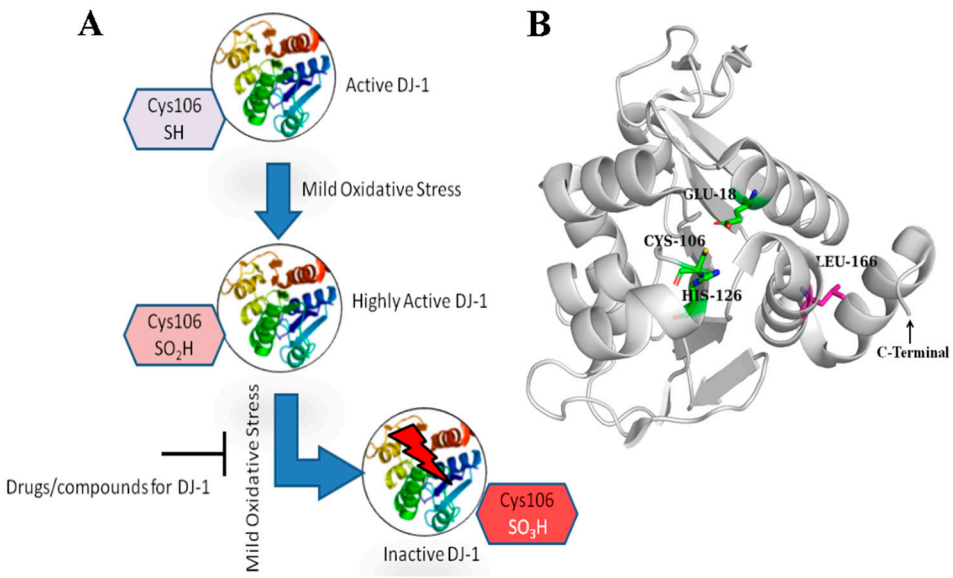


**Figure 1.** (**A**) Compounds targeting DJ-1 can enhance its activity or stabilize its active form, thereby promoting neuroprotection. (**B**) Crystallographic structure of DJ-1 monomer (PDB ID 6AFL). The important active site residues (Glu18, Cys106, and His126) are represented in the form of sticks in green color and labeled. The residue Leu166 mutation (L166P) in PD DJ-1 which disrupts the PD dimerization, is shown as pink sticks.

## 2. Materials and Methods

### *2.1. Receptor Structure*

The crystallographic structure of the DJ-1 protein was retrieved from the protein data bank (PDB) with the PDB id 6AFL (https://www.rcsb.org/structure/6AFL, accessed on 18 October 2024). This 1.6 Å resolution structure shows DJ-1 in its monomeric form, which was chosen for subsequent molecular docking and virtual screening. All other crystallographic molecules (water, ions, and any small molecules) were removed from the structure before proceeding with the docking experiments. AutoDock tools 1.5.6 [16] were used to prepare the structure for docking by computing Gasteiger charges and adding polar hydrogen. After this, the protein structure was saved in .pdbqt format for docking experiments.

### *2.2. Drug Library Preparation*

In this study, we used a library of FDA-approved drugs from the DrugBank (https://go.drugbank.com/ (accessed on 18 October 2024)) database for drug repurposing. All these drugs have their respective ADMET (absorption, distribution, metabolism, excretion, and toxicity) properties documented in the DrugBank database. ADMET are key pharmacokinetic properties used to evaluate the drug-likeness and safety of a compound. The drug library of 2900 drugs was prepared for docking experiments using AutoDock tools [17] by adding polar hydrogens. After this, Gasteiger charges were also computed for all the drugs. Later on, the drug molecules were saved in .pdbqt format for docking purposes as AutoDock Vina takes the input of receptor and ligand in .pdbqt format for docking.

### *2.3. Molecular Docking*

Molecular docking experiments were performed using AutoDock Vina (1.1.2 (11 May 2011)) [18]. Vina has been extensively validated and is widely used in the scientific

community for docking studies, providing a reliable and well-documented tool for assessing protein–ligand interactions [19–22]. For docking the ligands to the DJ-1, the grid box was centered on the active site with the x = 35.812, y = −12.23, and z = −10.14. The grid box was defined as 40 Å in each direction (x, y, and z) to properly encompass the active site and adjacent regions for ligand binding investigation. In order to validate the docking protocol, we redocked the crystallized ligand (5-fluoranyl-1-(2-phenylethyl) indole-2,3-dione) bound with 6AFL. Two types of docking experiments were performed. In the first type of docking experiment, the whole protein was treated as rigid, and only the ligands were allowed to be flexible. Meanwhile, in the second type of docking experiment, the active site residues of the protein were treated flexibly. By allowing the active site residues to change conformations, we could better accommodate potential ligands and investigate how they fit into the pocket, particularly in cases where deeper interactions were necessary to stabilize the ligand within the shallow binding site. After the docking experiments, the drugs were ranked based on the binding energy scores (kcal/mol) assigned by Autodock Vina to each docked drug. Based on the binding scores and interactions, three drugs were chosen for further validation.

### 2.4. Prediction of Activity Spectra for Substances (PASS)

PASS analysis was performed to access the biological activities of the selected compounds using the PASS online web-based server (https://www.way2drug.com/PassOnline/index.php (accessed on 18 October 2024)). PASS is a computer method that predicts the pharmacological activity of drugs with around 95% accuracy. It employs structure-activity relationship (SAR) analysis, which draws on a training set of approximately 260,000 druglike compounds with reported biological activities. The predicted activities are displayed as a spectrum of activity, with two probabilities: likely activity (Pa) and probable inactivity (Pi), both ranging from 0.000 to 1.000. Typically, a molecule is regarded as potentially active for certain pharmacological activity if Pa > Pi, albeit the total of Pa and Pi does not always equal 1. Only molecules with a higher Pa value than Pi are considered feasible candidates for a specific biological activity [23].

### 2.5. Molecular Dynamics Simulations (MDSs)

Molecular dynamics simulation (MDS) is an in silico technique used for modeling the dynamic behavior and mechanism of drug and protein complexes. In this study GROMACS -2021 [24] was utilized to simulate the drug and protein complexes acquired from docking experiments. Charmm36-jul2022 [25] and CGENFF server 4.6 [26] were utilized to construct protein and ligand topology, respectively. The TIP3P water model was utilized to solvate the systems, maintaining a distance of 1.0nm between the solvated system and the edges of the box. After this, the systems were neutralized by adding ions, and energy minimization of the systems was performed using 1000 steps of the steepest descent method. The temperature of the systems was equilibrated for 300 ps at 300 K. The systems were further equilibrated using an NPT ensemble at 300 K, with position restraints applied to both the protein and ligand to stabilize the complex. LINCS constraints were applied to all the bonded interactions.

After this, a simulation of 100 ns for each system was performed with a step size of 2 fs/step. After the simulations, RMSD, RMSF, PCA, and MMPBSA analyses were conducted using the gromacs different analysis modules.

### 2.6. Binding Energy (MMPBSA)

The molecular MMPBSA technique was used to calculate the binding free energy of the protein and drugs. To estimate the free energy of binding, this approach integrates molecular mechanics with continuum solvation models. The MM/PBSA calculations

were carried out utilizing trajectories taken from the last 20 ns of the molecular dynamics trajectories. These calculations were performed using the gmx_MMPBSA module to analyze the trajectory data, giving insights into the stability and strength of the protein–ligand interactions. The binding free energy is typically the sum of the enthalpy of binding and conformational entropy after ligand binding. Gmx_MMPBSA estimates the binding energy $\Delta G_{binding}$ as follows:

$$\Delta G_{binding} = \Delta G_{Complex} - \left(\Delta G_{Protein} + \Delta G_{Ligand}\right) \quad (1)$$

In Equation (1), each term on the right is given by $G_x = \Delta E_{MM} + \Delta E_{solv} - T\Delta S$. In turn, it can be expressed as follows:

$$\Delta G_{binding} = \Delta E_{MM} + \Delta E_{solv} - T\Delta S \quad (2)$$

In Equation (2), $\Delta E_{MM} + \Delta E_{solv}$ corresponds to the enthalpic binding.

$\Delta E_{MM}$ is the molecular mechanic energy, which consists of non-bonded energy electrostatics ΔEelec and van der Waals interactions ΔEvdw, and bonded energy, also known as internal energy, which includes angle bending, bond stretching, and torsional interaction.

Meanwhile, $\Delta E_{solv}$ in Equation (2) is solvation free energy, consisting of polar solvation (ΔEGB) and non-polar solvation energy (ΔESURF).

$$\Delta E_{solv} = \Delta EGB + \Delta ESURF \quad (3)$$

The $-T\Delta S$ in Equation (2) is the entropic contribution [27]. The MMPBSA approach calculates effective binding energies by omitting the entropic term, $-T\Delta S$. When the entropic term is excluded, the estimated value is the effective free energy, which is generally adequate for comparing the binding free energies of related ligands. The term '$-T\Delta S$' represents the changes in conformational entropy following ligand binding, which are generally obtained through normal mode analysis on a collection of conformations derived from MD simulations. However, when only the relative binding free energy of similar ligands is needed, the change in conformational entropy can usually be ignored.

## 3. Results

### *3.1. Docking Protocol Validation*

In order to validate the predictive ability of the Autodock Vina docking protocol, the native cocrystallized ligand (5-fluoranyl-1-(2-phenylethyl) indole-2,3-dione) was redocked to the DJ-1 (PDB ID: 6AFL). The native ligand was extracted from the binding pocket and then redocked using the same docking parameters used for subsequent screening. The accuracy of the docking was evaluated by comparing the redocked pose with the experimental binding conformation. The redocked conformation of the native ligand superimposed to the cocrystallized ligand is represented in Figure 2. The binding score of the redocked conformation of the reference ligand was −5.92 kcal/mol. The RMSD valued for the redocked ligand superimposed to the cocrystallized ligand was 2.0 Å, which is within the widely accepted threshold for accurate pose reproduction in docking studies [28].

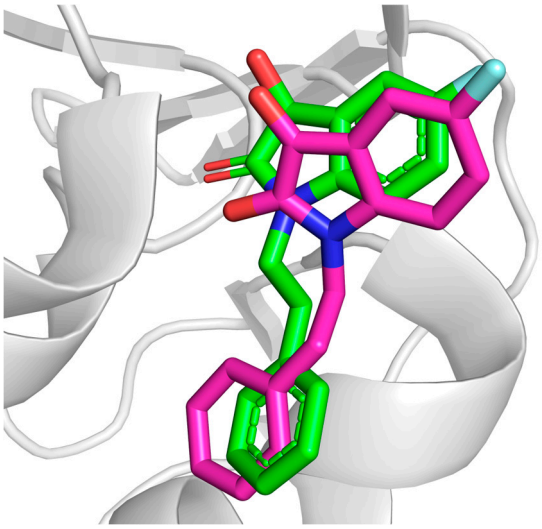

**Figure 2.** Redocked conformation of the native ligand (pink) superimposed to cocrystallized conformation (green).

### *3.2. Molecular Docking and Interaction Analysis*

A library consisting of 2900 drug-like compounds sourced from DrugBank was screened through molecular docking against the DJ-1 protein. Following the docking procedure, the compounds were ranked based on their binding affinities. From this initial ranking, we selected the top 20 drugs for further analysis. These top-ranking drugs were again flexibly docked to allow for more accurate predictions by accommodating the flexibility of the key residues in the active site. After flexible docking, the compounds were visually analyzed. Compounds interacting with the critical residues Cys106, Asn76, Glu18, and Gly75, which are known to play significant roles in DJ-1's biological function, were selected for further analysis. Three compounds droxicam, pteroylglutamic acid, and niraparib were identified as forming stable complexes with DJ-1. Interactions and binding energy scores of these three drugs are presented in Table 1. This stability was supported by their favorable binding scores and the formation of key interactions with the critical residues, suggesting these compounds may serve as promising candidates for further study as DJ-1 inhibitors. Droxicam formed hydrogen bonds with the side-chains atoms of the four residues—Cys106, Arg46, Asn76, and Glu15 with a binding energy score of −7.6 kcal/mol. Pteroylglutamic acid formed hydrogen bonds with the residues Ser47, Asn76, and Cys106 with a binding energy score of −7.6 kcal/mol, indicating strong polar interactions. Niraparib demonstrates strong hydrophobic interactions, particularly with Leu77 and Arg48, and hydrogen bonds with Asn76, Gln45, and Asp49 with a binding energy score of −7.5 kcal/mol. All three compounds—droxicam, pteroylglutamic acid, and niraparib—demonstrated significant interactions with the crucial residues Glu18, Gly75, Cys106, and Arg48, which are essential for the function of DJ-1. These interactions suggest that the compounds may effectively modulate or inhibit DJ-1's activity, making them promising candidates for further development as therapeutic agents. Figures 3 and 4 demonstrate the 3D and 2D interactions between the drugs and DJ-1 protein and the physiochemical properties of the three candidate compounds are described in Table 2.

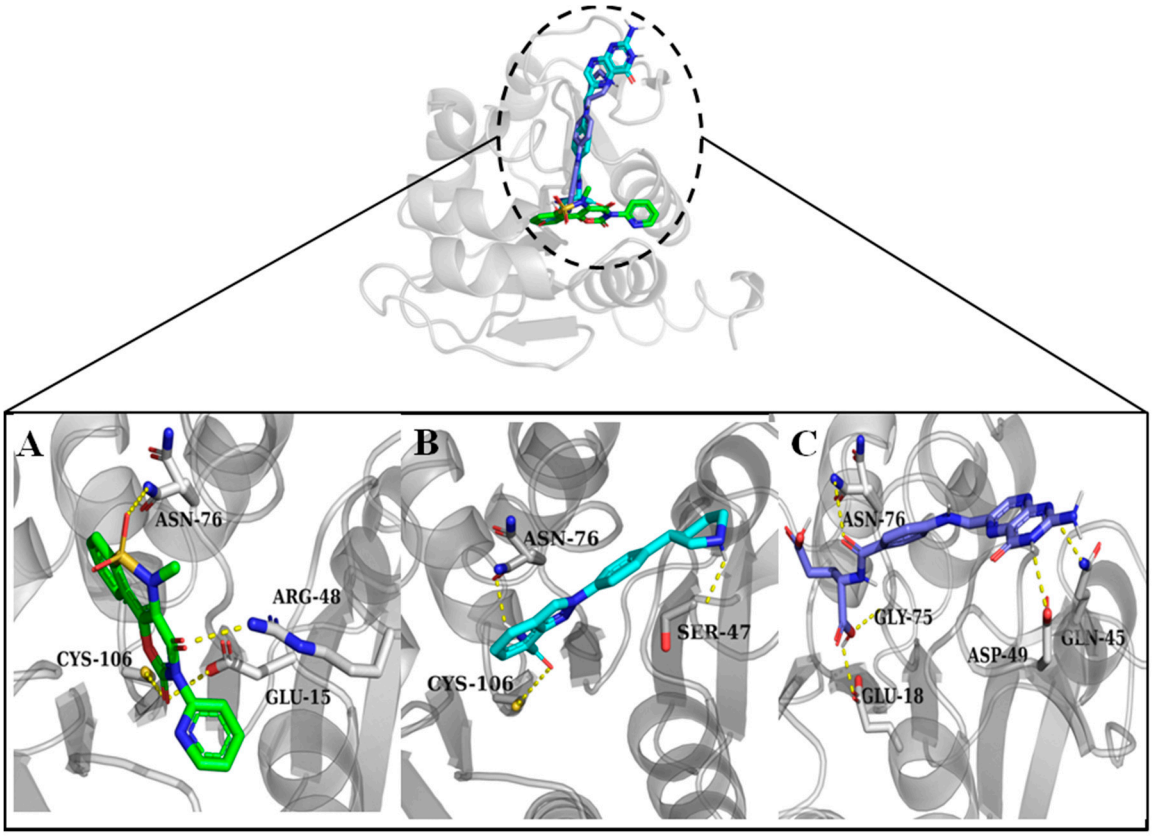


**Figure 3.** Hydrogen bond interactions between the compounds and DJ-1 active site residues. Residues forming the hydrogen bonds are shown as sticks. (**A**) Droxicam, (**B**) niraparib, and (**C**) pteroylglutamic acid.

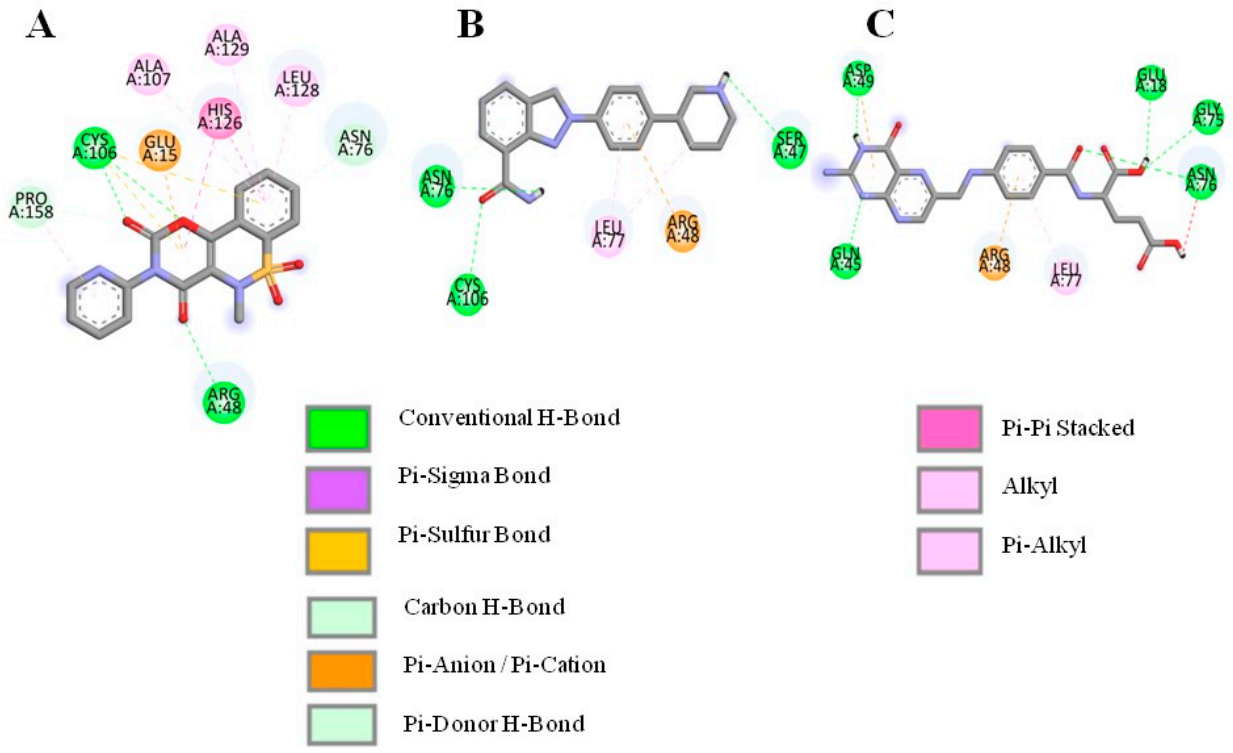


**Figure 4.** D interactions between the selected compounds and the active residue of DJ-1. (**A**) Droxicam, (**B**) niraparib and (**C**) pteroylglutamic acid.

**Table 1.** Interacting residues of DJ-1 that form hydrogen bonds and other interactions, and the binding energy scores of the selected drugs.

| Drug Name | Drug Bank Ids | Binding Score (Kcal/mol) | Hydrogen Bond Interactions | Other Interactions |
|---|---|---|---|---|
| Droxicam | DB09215 | −7.6 | Cys106, Arg48, Asn76, Glu15 | His126, Pro158, Leu128, Ala129, Ala107 |
| Niraparib | DB11793 | −7.6 | Ser47, Asn76, Cys106 | Leu77, Arg48 |
| Pteroylglutamic Acid | DB00158 | −7.5 | Gln45, Asp49, Glu18, Gly75, Asn76 | Arg48, Leu77 |

**Table 2.** Physiochemical properties of the selected compounds.

| Drug Name | Chemical Structure | MolWT (g/mol) | LogP | H-Bond Donors | H-Bond Acceptors |
|---|---|---|---|---|---|
| Reference | 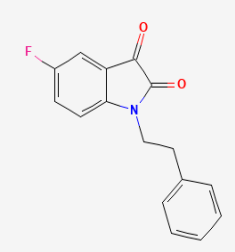 | 269.27 | 3 | 0 | 3 |
| Droxicam | 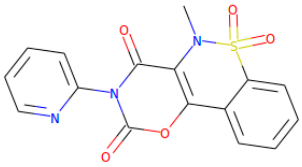 | 357.3 | 0.99 | 0 | 7 |
| Pteroylglutamic Acid | 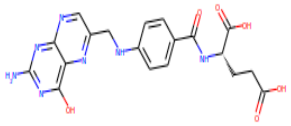 | 441.4 | 0.368 | 6 | 10 |
| Niraparib | 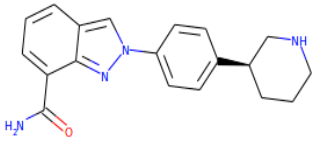 | 320.4 | 2.591 | 3 | 3 |

### *3.3. PASS Online Analysis of Compounds Against Parkinson's Disease*

The potential biological activities of the selected compounds were estimated using the PASS online webserver. This tool predicts various biological activities in the human body by calculating the probable activity (Pa) and probable inactivity (Pi) for each compound. The activities relating to Pa > Pi values are presented in Table 3. These results indicate a range of biological properties, including roles in neurodegenerative diseases, enzyme inhibition, and anti-inflammatory effects. Niraparib demonstrated high efficacy as a poly(ADP-ribose) polymerase inhibitor with a Pa value of 0.752 and as a nootropic with a Pa value of 0.755. It also showed activity for neurological disease therapy with a Pa value of 0.38 and antineoplastic enhancement with a Pa value of 0.459. Pteroylglutamic acid is a powerful gamma-glutamyl hydrolase inhibitor (Pa = 0.632), immunostimulant (Pa = 0.576), and thiol oxidase inhibitor (Pa = 0.575). It also has activity in treating autoimmune diseases

(Pa = 0.318) and inhibiting MAP3K5 (Pa = 0.371). Droxicam had the highest activity for neurodegenerative disease therapy (Pa = 0.490) and nootropic characteristics. It also showed activities including antiparkinsonian (Pa = 0.372), anti-inflammatory (Pa = 0.472), and anxiolytic (Pa = 0.370).

**Table 3.** Biological activities of the candidate ligands predicted by PASS online server. Pa is probable activity and Pi is probable inactivity.

| Compound Name | Activity | Pa | Pi |
|---|---|---|---|
| Niraparib | Poly(ADP-ribose) polymerase inhibitor | 0.752 | 0.003 |
| | Nootropic | 0.755 | 0.026 |
| | MAP kinase kinase 4 inhibitor | 0.390 | 0.006 |
| | Neurodegenerative diseases treatment | 0.381 | 0.081 |
| | Antiinflammatory, ophthalmic | | |
| | Antineoplastic enhancer | 0.459 | 0.013 |
| | Anticonvulsant | 0.376 | 0.075 |
| | Antineurogenic pain | 0.238 | 0.144 |
| | Anti-neurotic | 0.303 | 0.244 |
| | Lysyl oxidase inhibitor | 0.226 | 0.204 |
| Pteroylglutamic Acid | Gamma-glutamyl hydrolase inhibitor | 0.632 | 0.000 |
| | Immunostimulant | 0.576 | 0.026 |
| | Autoimmune disorders treatment | 0.318 | 0.089 |
| | MAP3K5 inhibitor | 0.371 | 0.042 |
| | Thiol oxidase inhibitor | 0.575 | 0.014 |
| Droxicam | Antiparkinsonian | 0.372 | 0.036 |
| | Neurodegenerative diseases treatment | 0.490 | 0.034 |
| | Anxiolytic | 0.370 | 0.047 |
| | Nootropic | 0.497 | 0.131 |
| | Anti-inflammatory | 0.472 | 0.065 |
| | Anti-neurotic | 0.460 | 0.1294 |
| | Non-steroidal anti-inflammatory agent | 0.394 | 0.106 |
| | S)-6-hydroxynicotine oxidase inhibitor | 0.345 | 0.078 |
| | Chloride peroxidase inhibitor | 0.365 | 0.127 |
| | Hydroxylamine oxidase inhibitor | 0.439 | 0.119 |

### *3.4. Molecular Dynamics Simulations (MDSs)*

Molecular dynamics simulations are a fundamental method in computational biology, used to study the detailed movements and behaviors of proteins and other macromolecules over time. MDSs model the system at an atomic level, treating all components, such as ligands, proteins, and solvent molecules if using explicit water, as fully flexible. This flexibility allows MDSs to capture the dynamic behavior of molecular interactions and conformational changes, from rapid vibrations and rotations to slower processes like folding and complex formation [29,30].

### *3.5. Root Mean Square Deviations (RMSDs)*

RMSD is a useful metric for assessing the structural stability of protein–ligand complexes in molecular dynamics simulations. It determines the average movement of atoms in the complex over time. Lower and more consistent RMSD values often suggest that the protein–ligand complex is in a stable conformation throughout the simulation. This stability is critical for verifying the potential efficacy and behavior of ligands in binding assays since it indicates that the ligand is still well-positioned to engage consistently with the target protein's active region. Figure 5 shows the RMSD of all the simulated systems over a time of 100 ns. The apo DJ-1 form has an average RMSD of 0.21 nm, showing moderate stability and no notable structural abnormalities. Droxicam complex initially showed low RMSD values (0.17 nm) for the first 50 ns, reflecting stable binding. However, after 50 ns, the RMSD gradually increased to 0.23 nm, signaling minor structural changes while still maintaining overall stability. This increase in the fluctuations might be due to conformational changes that occurred in regions D42-P54 and D131-G136 (Figure 6). Region D42-P54 undergoes structural transition from beta sheets to loops, contributing to the high RMSD values in this complex. This region also exhibited some shifts in pteroylglutamic acid and niraparib (Figure 7), indicating that this region remained quite flexible during the simulations. Pteroylglutamic acid had the smallest and most constant RMSD (0.12 nm), indicating a highly stable interaction with minimal fluctuations during the simulation. Niraparib, on the other hand, showed larger variations at first, with an RMSD peak at 0.3 nm within the first 30 ns, indicating early structural changes. Later, the complex stabilized at about 0.2 nm, indicating that once equilibrated, the binding between Niraparib and DJ-1 is stable. Overall, these results suggest that pteroylglutamic acid exhibits the strongest binding stability, followed by niraparib after its initial fluctuations, while droxicam maintains stability despite minor adjustments over time.

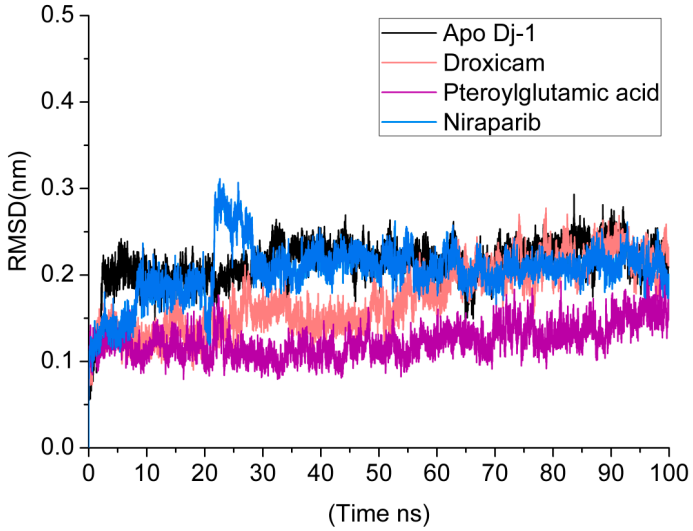


**Figure 5.** RMSD analysis over a 100 ns Molecular dynamics (MDs) simulation for the DJ-1 protein in its apo form and in complex with three ligands: droxicam, pteroylglutamic acid, and niraparib.

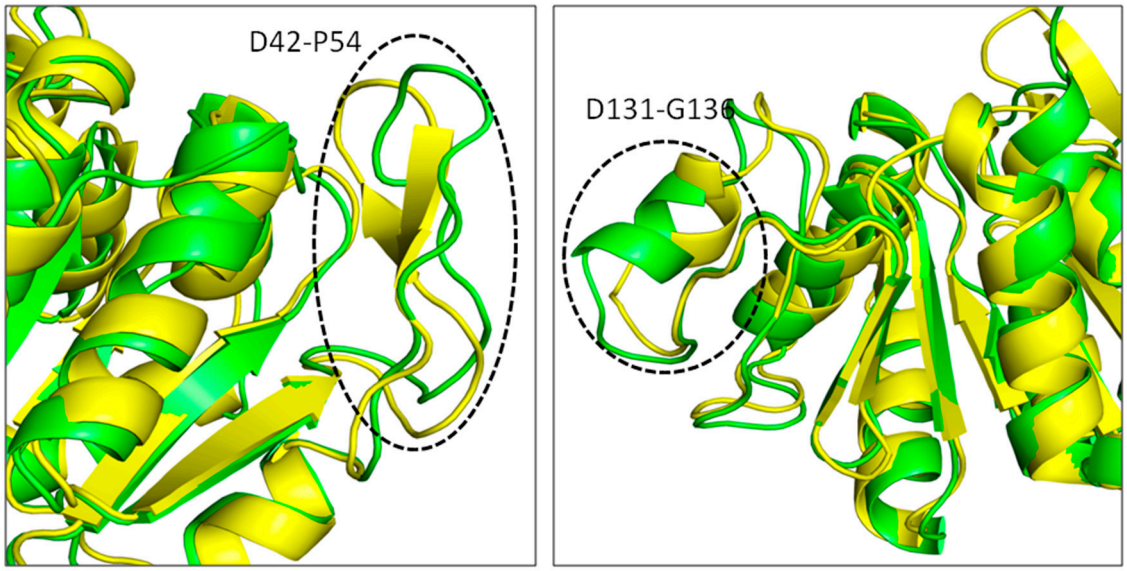


**Figure 6.** Conformational changes occurred in the DJ–1 structure complexed with droxicam compound. Structure extracted at 100 ns in green superimposed to 0 ns yellow.

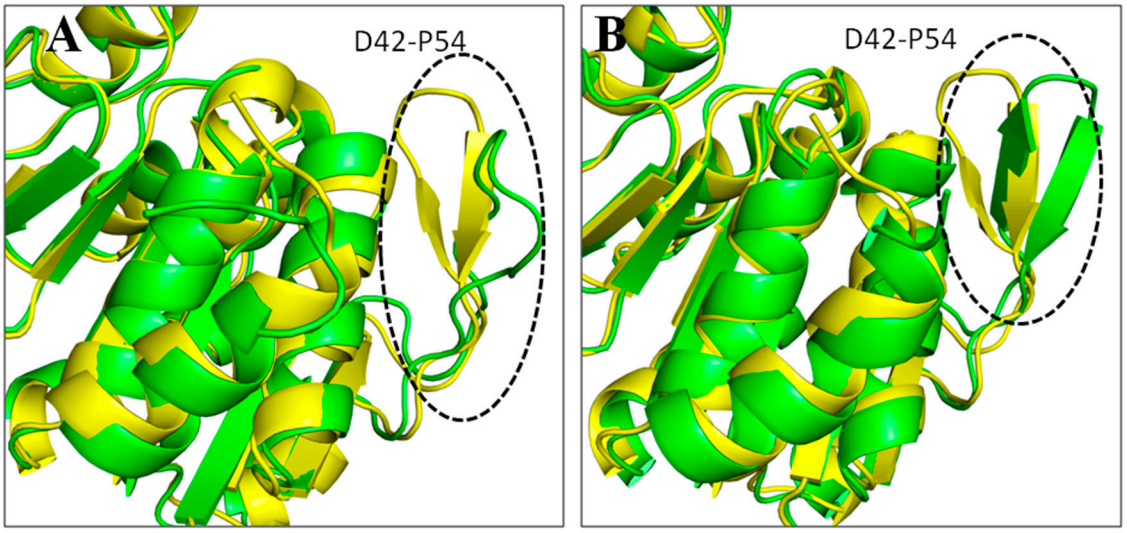


**Figure 7.** Conformational changes occurred in the DJ–1 structure complexed with pteroylglutamic acid (**A**) and niraparib (**B**). Structure extracted at 100 ns in green superimposed to 0 ns yellow.

### *3.6. Root Mean Square Fluctuations (RMSF)*

The RMSF provides a detailed view of the flexibility of individual residues in the protein over the simulation time. Residues with higher RMSF values indicate regions of greater flexibility, while lower values correspond to more rigid, stable regions. In the apo form, certain regions of the protein display higher RMSF values, signifying increased flexibility in the absence of a bound ligand. Upon binding to pteroylglutamic acid, RMSF values significantly dropped in areas close to the binding pocket and in residues that interacted with the ligand. This reduction in RMSF values implies that these regions are stabilized by ligand interaction, which reduces their conformational freedom. In comparison to the apo form and other complexes, the RMSF values for the droxicam and DJ-1 complex were higher in certain locations, particularly noticeable in several residues within the active site. As can be seen from the figure, this complex shows higher RMSF values for Glu15, Arg48, Ser47, Gly75, and Asn76 than the other two complexes and the apo form. With an average RMSF value of 0.12 nm, this greater flexibility shows that even

though droxicam binds to the protein, it permits greater mobility in specific areas. In the case of the niraparib complex, the RMSF values are lower (average 0.10 nm) than in the apo state. This reduction in flexibility, like that observed with pteroylglutamic acid, points to a stabilizing effect, particularly around the binding site, where the ligand tightly interacts with the protein. Figure 8 represents the RMSF of all the simulated systems. Overall, the RMSF analysis revealed that ligand binding reduced the flexibility of certain protein regions, particularly those involved in direct ligand interactions or within the binding pocket (Figure 9). Gln45 in niraparib exhibits higher fluctuations than the apo and other complexes. This increased flexibility could be attributed to the lack of direct interactions between niraparib and Gln45. This stabilization is crucial for the protein's structural and functional integrity. However, some peaks remain present in the RMSF plots across all simulated systems, particularly in the region C46–V50, indicating regions that undergo significant conformational changes. Additionally, the RMSF results were consistent with the RMSD results.

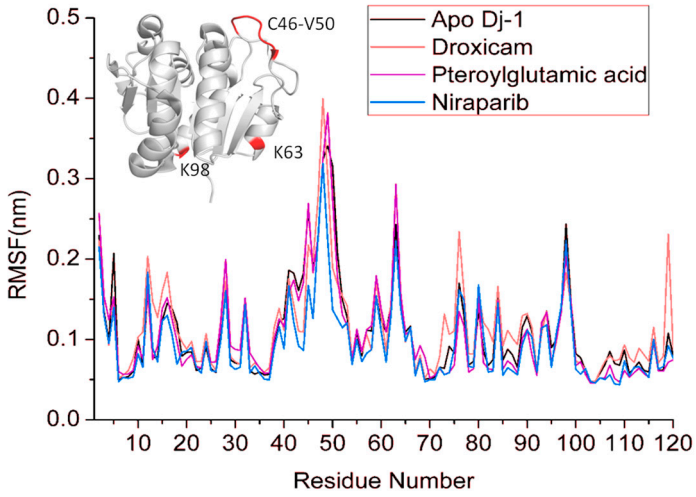


**Figure 8.** RMSF of the apo DJ–1 and drug bound states for 100ns simulation time. Fluctuating regions of the DJ-1 are shown in red, and residues are labeled.

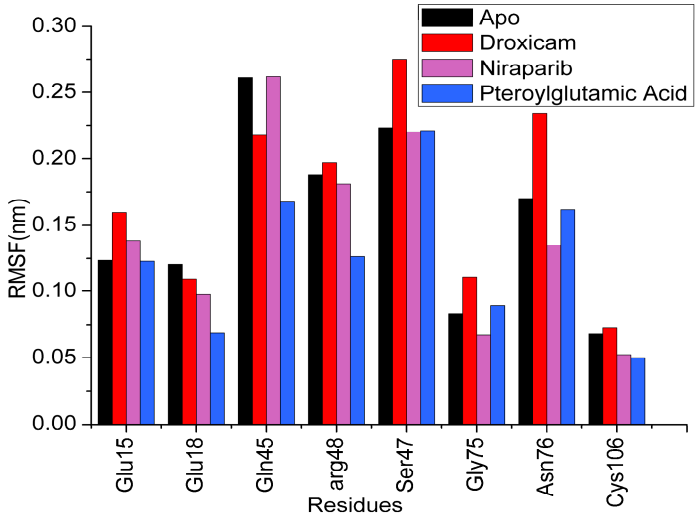


**Figure 9.** RMSF values of the crucial active site residues of apo and three ligand complexes.

### *3.7. Principal Component Analysis*

PCA is used to determine the global movements of proteins. It lowers the complex trajectory data to principal components (PCs), which highlight the protein's most significant

motions. This allows us to compare the overall conformational space sampled by the protein in both its apo and complex forms. Figure 10 shows the PCA plots of all the simulated systems. The PCA plot for the apo form demonstrates a larger range of conformations than the complexes suggesting that without ligands, DJ-1 is more flexible and can explore a wider range of conformational states. The conformational space of droxicam is more concentrated than the apo form. This demonstrated that the protein DJ-1 adopts fewer conformations when bound to droxicam, implying that ligand binding limits the DJ-1's flexibility. The PCA plot for complex pteroylglutamic acid displayed a conformational landscape distinct from complex droxicam. However, the spread remains less than in the apo version. Most notably, complex niraparib showed a tightly packed distribution, implying a stable conformational state with low structural variations during the simulation. This finding agrees with the RMSD and RMSF analyses. Each ligand causes a distinct conformational landscape, emphasizing its impacts on the protein's overall dynamics.

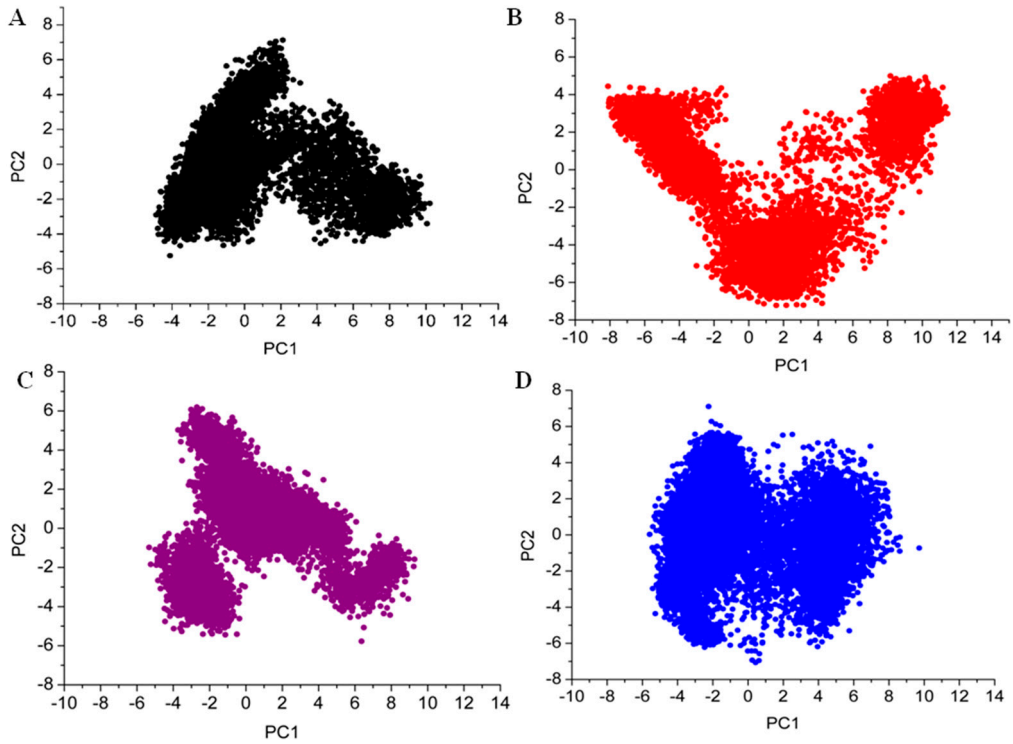


**Figure 10.** The distribution of data among the first two principal components (PC1 and PC2) of three complexes is represented using Principal Component Analysis (PCA) plots (**A**) apo, (**B**) droxicam, (**C**) pteroylglutamic acid, and (**D**) niraparib.

### *3.8. MMPBSA Analysis*

The MMPBSA approach is widely used as a dependable and effective tool for computing free energy in protein–ligand interaction simulations [31]. Binding free energies obtained using MMPBSA were utilized to validate the results of docking and simulation results, providing more information about the binding affinities of compounds with target DJ-1. For this study, the binding free energies were calculated using the last 20 ns of the 100 ns simulation trajectory. The average binding free energies of the complexes are shown in Table 4. Niraparib exhibited a strong binding affinity of −13.50 kcal/mol with the DJ-1, followed by pteroylglutamic acid. Larger negative values indicate stronger interactions between the compound and the protein. Additionally, niraparib shows a much larger negative electrostatic energy, and vdw interactions suggesting strong favorable electrostatic interactions, while the other compounds display weaker electrostatic contributions. In the gas phase (without solvation), niraparib demonstrates the most favorable binding,

highlighting its strong overall non-covalent interactions. The solvation energy for niraparib was the highest among all; however, despite its highest solvation energy being the strongest binding overall. After niraparib, pteroylglutamic acid showed a good binding affinity of −11.41 kcal/mol with DJ-1. The ΔEvdw and ΔEelec participated most, contributing favorably to the overall binding. Droxicam has the weakest binding affinity, with minimal van der Waals and electrostatic interactions and a lower solvation penalty.

**Table 4.** Binding free energies of DJ-1 in complex with three drugs. The table provides the energy contributions (in kcal/mol) for each energy term. ΔEvdw: van der Waals, ΔEelec: electrostatic, ΔESURF: non-polar solvation energy, ΔEGB: polar solvation energy. ΔGSOLV: polar and non-polar contribution from polar solvation. ΔGGAS: total gas phase energy combining Δ Evdw and ΔEelec in the absence of solvation effect, ΔTOTAL: overall binding free energy (ΔTOTAL = ΔGSOLV+ ΔGGAS=, ΔGGAS = Δ Evdw+ ΔEelec, ΔGSOLV = ΔESURF+ ΔEGB).

| Energy Terms (Kcal/mol) | Droxicam | Pteroylglutamic Acid | Niraparib |
|---|---|---|---|
| ΔEvdw | −5.20 | −18.79 | −20.18 |
| ΔEelec | −3.74 | −5.06 | −52.51 |
| ΔESURF | −0.80 | −2.60 | −3.64 |
| ΔEGB | 6.57 | 15.04 | 62.84 |
| ΔGSOLV | 5.78 | 12.45 | 59.20 |
| ΔGGAS | −8.66 | −23.86 | −72.70 |
| ΔTOTAL | −2.88 | −11.41 | −13.50 |

## 4. Discussion

In this study, we aimed to identify potential DJ-1 modulators for Parkinson's disease (PD) through a drug repurposing approach. By screening 2900 FDA-approved drugs, we identified 3 promising compounds: droxicam, pteroylglutamic acid, and niraparib. These compounds were selected based on their strong binding affinities to the DJ-1 protein active site, with docking scores ranging from −7.6 to −7.5 kcal/mol. The importance of these interactions, particularly with the critical residue Cys106, Gly75, Asn76, and Glu18 highlights their potential to modulate DJ-1 activity and mitigate oxidative stress, a key factor in PD pathology. Tashiro et al. discovered and optimized various inhibitors of DJ-1 making interactions with residue Cys106, Ans76, Glu18, and Gly75, highlighting the implication of these residues in drug binding [32]. MDSs were further employed to assess the dynamic behavior of the DJ-1 complexed with drugs by calculating RMSD and RMSF. Small RMSD values are commonly assumed to imply a stable state of the system, whereas large RMSD values imply major conformational changes in the investigated system [33]. The RMSD values and RMSF analysis revealed that pteroylglutamic acid and niraparib exhibited stability inside the DJ-1 active site, indicating stable complex [34].

MMPBSA binding energy analysis validated the computational findings by highlighting niraparib (−13.50 kcal/mol) and pteroylglutamic acid (−11.41 kcal/mol) as the most favorable compounds in terms of binding free energy. A lower binding free energy indicates a better affinity between the drug and protein, which is essential for effective inhibition [35]. This suggests that pteroylglutamic acid and niraparib could be a strong candidate for further investigation. Notably, pteroylglutamic acid commonly known as folic acid) has been studied in the context of neurodegenerative illnesses due to its ability to lower homocysteine levels and battle oxidative stress [36]. According to research, folic acid may help improve cognitive functioning, especially in the elderly and people with mild cognitive impairment (MCI) [37]. Clinical investigations have shown that folic acid

supplementation can decrease cognitive deterioration and prevent brain atrophy in people with MCI. These findings highlight the importance of folic acid as a crucial nutrient in maintaining brain health and cognitive function in older populations [38,39]. On the other hand, niraparib is licensed for treating recurrent ovarian cancer and is expected to be approved for more disease indications [40]. In silico experiments provide information about the potential binding patterns and stability of the drugs; however, they are not reliable indicators of biological activity. Further experimental validation is needed to determine the biological efficacy of these drugs.

## 5. Conclusions

The goal of this work was to find potential inhibitors of the DJ-1 protein utilizing a drug-repurposing method. To assess DJ-1 binding affinities, we screened 2900 FDA-approved drugs using molecular docking. Droxicam, pteroylglutamic acid, and niraparib were chosen as the top candidates due to their high docking scores and strong interactions with DJ-1 key residues, particularly Cys106, Glu18, and His126. These residues are critical to DJ-1's ability to protect against oxidative stress, a major contributor to the pathogenesis of PD. Moreover, MDSs were performed to analyze the dynamic behavior and validate the stability of the complexes and apo DJ-1. Two of the three drugs, pteroylglutamic acid and niraparib, displayed good stability throughout 100ns simulations, indicating therapeutic potential. MMPBSA confirmed that pteroylglutamic acid and niraparib are the most promising inhibitors because of their strong binding affinity. Conclusively, MDS and MMPBSA analyses revealed pteroylglutamic acid and niraparib as potential inhibitors of the DJ-1 protein with strong binding affinities and favorable interactions with the crucial residues. Our findings provide a foundation for further experimental validation and optimization of these drugs.

**Author Contributions:** Conceptualization, A.A.; methodology, T.A. and A.A.; software, A.A.; validation, T.A. and A.A.; formal analysis, T.A. and A.A.; investigation, T.A. and A.A.; resources, A.A.; data curation, T.A.; writing—original draft preparation, T.A.; writing—review and editing, A.A.; visualization, T.A.; supervision, A.A.; project administration, A.A.; funding acquisition, A.A. All authors have read and agreed to the published version of the manuscript.

**Funding:** This research was funded by Prince Sattam bin Abdulaziz University project number (PSAU/2024/03/31735).

**Data Availability Statement:** All the data used in this study is available publicly and within the article.

**Acknowledgments:** The authors extend their appreciation to the Deputyship for Research and Innovation, Ministry of Education in Saudi Arabia for funding this research. This study is supported via funding from the Prince Sattam bin Abdulaziz University project number (PSAU/2024/03/31735).

**Conflicts of Interest:** The authors declare no conflicts of interest.

## References

1. Schapira, A.H.; Jenner, P. Etiology and pathogenesis of Parkinson's disease. *Mov. Disord.* **2011**, *26*, 1049–1055. [CrossRef] [PubMed]
2. Martin, I.; Dawson, V.L.; Dawson, T.M. Recent advances in the genetics of Parkinson's disease. *Annu. Rev. Genom. Hum. Genet.* **2011**, *12*, 301–325. [CrossRef] [PubMed]
3. Kouli, A.; Torsney, K.M.; Kuan, W.-L. *Parkinson's Disease: Etiology, Neuropathology, and Pathogenesis*; Codon Publications: Brisbane, Australia, 2018; pp. 3–26.
4. Bonifati, V.; Rizzu, P.; Van Baren, M.J.; Schaap, O.; Breedveld, G.J.; Krieger, E.; Dekker, M.C.; Squitieri, F.; Ibanez, P.; Joosse, M. Mutations in the DJ-1 gene associated with autosomal recessive early-onset parkinsonism. *Science* **2003**, *299*, 256–259. [CrossRef]
5. Hijioka, M.; Inden, M.; Yanagisawa, D.; Kitamura, Y. DJ-1/PARK7: A new therapeutic target for neurodegenerative disorders. *Biol. Pharm. Bull.* **2017**, *40*, 548–552. [CrossRef]

6. Gao, H.; Yang, W.; Qi, Z.; Lu, L.; Duan, C.; Zhao, C.; Yang, H. DJ-1 protects dopaminergic neurons against rotenone-induced apoptosis by enhancing ERK-dependent mitophagy. *J. Mol. Biol.* **2012**, *423*, 232–248. [CrossRef]
7. Honbou, K.; Suzuki, N.N.; Horiuchi, M.; Niki, T.; Taira, T.; Ariga, H.; Inagaki, F. The crystal structure of DJ-1, a protein related to male fertility and Parkinson's disease. *J. Biol. Chem.* **2003**, *278*, 31380–31384. [CrossRef]
8. Lee, S.J. Crystal structures of human DJ-1 and Escherichia coli Hsp31, which share an evolutionarily conserved domain. *J. Biol. Chem.* **2003**, *278*, 44552–44559. [CrossRef]
9. Tao, X.; Tong, L. Crystal structure of human DJ-1, a protein associated with early onset Parkinson's disease. *J. Biol. Chem.* **2003**, *278*, 31372–31379. [CrossRef]
10. Gautier, V.; Le, H.-T.; Malki, A.; Messaoudi, N.; Caldas, T.; Kthiri, F.; Landoulsi, A.; Richarme, G. YajL, the prokaryotic homolog of the Parkinsonism-associated protein DJ-1, protects cells against protein sulfenylation. *J. Mol. Biol.* **2012**, *421*, 662–670. [CrossRef]
11. Olzmann, J.A.; Brown, K.; Wilkinson, K.D.; Rees, H.D.; Huai, Q.; Ke, H.; Levey, A.I.; Li, L.; Chin, L.-S. Familial Parkinson's disease-associated L166P mutation disrupts DJ-1 protein folding and function. *J. Biol. Chem.* **2004**, *279*, 8506–8515. [CrossRef]
12. Repici, M.; Giorgini, F. DJ-1 in Parkinson's disease: Clinical insights and therapeutic perspectives. *J. Clin. Med.* **2019**, *8*, 1377. [CrossRef] [PubMed]
13. Parvathaneni, V.; Kulkarni, N.S.; Muth, A.; Gupta, V. Drug repurposing: A promising tool to accelerate the drug discovery process. *Drug Discov. Today* **2019**, *24*, 2076–2085. [CrossRef] [PubMed]
14. Huang, M.; Chen, S. DJ-1 in neurodegenerative diseases: Pathogenesis and clinical application. *Prog. Neurobiol.* **2021**, *204*, 102114. [CrossRef] [PubMed]
15. Athauda, D.; Maclagan, K.; Skene, S.S.; Bajwa-Joseph, M.; Letchford, D.; Chowdhury, K.; Hibbert, S.; Budnik, N.; Zampedri, L.; Dickson, J. Exenatide once weekly versus placebo in Parkinson's disease: A randomised, double-blind, placebo-controlled trial. *Lancet* **2017**, *390*, 1664–1675. [CrossRef]
16. Pacheco, A.B.; Hpc, L. *Introduction to AutoDock and AutoDock Tools*; Louisiana State University: Baton Rouge, LA, USA, 2012.
17. Ravi, L.; Kannabiran, K. A handbook on protein-ligand docking tool: AutoDock 4. *Innovare J. Med. Sci.* **2016**, 28–33. Available online: https://www.academia.edu/84591451/A_Handbook_on_Protein_Ligand_Docking_Tool_AutoDock_4 (accessed on 18 October 2024).
18. Trott, O.; Olson, A.J. AutoDock Vina: Improving the speed and accuracy of docking with a new scoring function, efficient optimization, and multithreading. *J. Comput. Chem.* **2010**, *31*, 455–461. [CrossRef]
19. Dong, R.; Huang, R.; Shi, X.; Xu, Z.; Mang, J. Exploration of the mechanism of luteolin against ischemic stroke based on network pharmacology, molecular docking and experimental verification. *Bioengineered* **2021**, *12*, 12274–12293. [CrossRef]
20. Zhu, J.; Wei, J.; Lin, Y.; Tang, Y.; Su, Z.; Li, L.; Liu, B.; Cai, X. Inhibition of IL-17 signaling in macrophages underlies the anti-arthritic effects of halofuginone hydrobromide: Network pharmacology, molecular docking, and experimental validation. *BMC Complement. Med. Ther.* **2024**, *24*, 105. [CrossRef]
21. Mellini, M.; Di Muzio, E.; D'Angelo, F.; Baldelli, V.; Ferrillo, S.; Visca, P.; Leoni, L.; Polticelli, F.; Rampioni, G. In silico selection and experimental validation of FDA-approved drugs as anti-quorum sensing agents. *Front. Microbiol.* **2019**, *10*, 2355. [CrossRef]
22. Muneer, I.; ul Qamar, M.T.; Tusleem, K.; Rauf, S.A.; Hussain, H.M.; Siddiqi, A.R. Discovery of selective inhibitors for cyclic AMP response element-binding protein: A combined ligand and structure-based resources pipeline. *Anti-Cancer Drugs* **2019**, *30*, 363–373. [CrossRef]
23. Lagunin, A.; Filimonov, D.; Poroikov, V. Multi-targeted natural products evaluation based on biological activity prediction with PASS. *Curr. Pharm. Des.* **2010**, *16*, 1703–1717. [CrossRef] [PubMed]
24. Bekker, H.; Berendsen, H.; Dijkstra, E.; Achterop, S.; Vondrumen, R.v.; Vanderspoel, D.; Sijbers, A.; Keegstra, H.; Renardus, M. Gromacs-a parallel computer for molecular-dynamics simulations. In Proceedings of the 4th international conference on computational physics (PC 92), Prague, Czech Republic, 24–28 August 1992; pp. 252–256.
25. Best, R.B.; Zhu, X.; Shim, J.; Lopes, P.E.; Mittal, J.; Feig, M.; MacKerell, A.D., Jr. Optimization of the additive CHARMM all-atom protein force field targeting improved sampling of the backbone $\phi$, $\psi$ and side-chain $\chi1$ and $\chi2$ dihedral angles. *J. Chem. Theory Comput.* **2012**, *8*, 3257–3273. [CrossRef] [PubMed]
26. Vanommeslaeghe, K.; MacKerell, A.D., Jr. Automation of the CHARMM General Force Field (CGenFF) I: Bond perception and atom typing. *J. Chem. Inf. Model.* **2012**, *52*, 3144–3154. [CrossRef] [PubMed]
27. Valdés-Tresanco, M.S.; Valdés-Tresanco, M.E.; Valiente, P.A.; Moreno, E. gmx_MMPBSA: A new tool to perform end-state free energy calculations with GROMACS. *J. Chem. Theory Comput.* **2021**, *17*, 6281–6291. [CrossRef]
28. Ramírez, D.; Caballero, J. Is it reliable to take the molecular docking top scoring position as the best solution without considering available structural data? *Molecules* **2018**, *23*, 1038. [CrossRef]
29. AlRawashdeh, S.; Barakat, K.H. Applications of molecular dynamics simulations in drug discovery. *Comput. Drug Discov. Des.* **2023**, *2714*, 127–141.
30. Bhat, S.S.; Sindhu, R.; Prasad, S.K. A Bioinformatics Approach Towards Plant-Based Anticancer Drug Discovery. In *Computational Approaches in Biotechnology and Bioinformatics*; CRC Press: Boca Raton, FL, USA, 2024; pp. 35–60.

31. Wang, C.; Greene, D.A.; Xiao, L.; Qi, R.; Luo, R. Recent developments and applications of the MMPBSA method. *Front. Mol. Biosci.* **2018**, *4*, 87. [CrossRef]
32. Tashiro, S.; Caaveiro, J.M.; Nakakido, M.; Tanabe, A.; Nagatoishi, S.; Tamura, Y.; Matsuda, N.; Liu, D.; Hoang, Q.Q.; Tsumoto, K.J.A. Discovery and optimization of inhibitors of the Parkinson's disease associated protein DJ-1. *ACS Chem. Biol.* **2018**, *13*, 2783–2793. [CrossRef]
33. Rungrotmongkol, T.; Nunthaboot, N.; Malaisree, M.; Kaiyawet, N.; Yotmanee, P.; Meeprasert, A.; Hannongbua, S. Molecular insight into the specific binding of ADP-ribose to the nsP3 macro domains of chikungunya and Venezuelan equine encephalitis viruses: Molecular dynamics simulations and free energy calculations. *J. Mol. Graph. Model.* **2010**, *29*, 347–353. [CrossRef]
34. Adelakun, N.; Obaseki, I.; Adeniyi, A.; Fapohunda, O.; Obaseki, E.; Omotuyi, O. Discovery of new promising USP14 inhibitors: Computational evaluation of the thumb-palm pocket. *J. Biomol. Struct. Dyn.* **2022**, *40*, 3060–3070. [CrossRef]
35. Yau, M.Q.; Emtage, A.L.; Chan, N.J.; Doughty, S.W.; Loo, J.S. Evaluating the performance of MM/PBSA for binding affinity prediction using class A GPCR crystal structures. *J. Comput.-Aided Mol. Des.* **2019**, *33*, 487–496. [CrossRef] [PubMed]
36. Zhang, X.; Bao, G.; Liu, D.; Yang, Y.; Li, X.; Cai, G.; Liu, Y.; Wu, Y. The association between folate and Alzheimer's disease: A systematic review and meta-analysis. *Front. Neurosci.* **2021**, *15*, 661198. [CrossRef]
37. Ma, F.; Wu, T.; Zhao, J.; Ji, L.; Song, A.; Zhang, M.; Huang, G. Plasma homocysteine and serum folate and vitamin B12 levels in mild cognitive impairment and Alzheimer's disease: A case-control study. *Nutrients* **2017**, *9*, 725. [CrossRef] [PubMed]
38. Ma, F.; Zhou, X.; Li, Q.; Zhao, J.; Song, A.; An, P.; Du, Y.; Xu, W.; Huang, G. Effects of folic acid and vitamin B12, alone and in combination on cognitive function and inflammatory factors in the elderly with mild cognitive impairment: A single-blind experimental design. *Curr. Alzheimer Res.* **2019**, *16*, 622–632. [CrossRef] [PubMed]
39. Douaud, G.; Refsum, H.; de Jager, C.A.; Jacoby, R.; Nichols, T.E.; Smith, S.M.; Smith, A.D. Preventing Alzheimer's disease-related gray matter atrophy by B-vitamin treatment. *Proc. Natl. Acad. Sci. USA* **2013**, *110*, 9523–9528. [CrossRef]
40. Mirza, M.R.; Monk, B.J.; Herrstedt, J.; Oza, A.M.; Mahner, S.; Redondo, A.; Fabbro, M.; Ledermann, J.A.; Lorusso, D.; Vergote, I. Niraparib maintenance therapy in platinum-sensitive, recurrent ovarian cancer. *New Engl. J. Med.* **2016**, *375*, 2154–2164. [CrossRef]


**Disclaimer/Publisher's Note:** The statements, opinions and data contained in all publications are solely those of the individual author(s) and contributor(s) and not of MDPI and/or the editor(s). MDPI and/or the editor(s) disclaim responsibility for any injury to people or property resulting from any ideas, methods, instructions or products referred to in the content.